# $^{238}$U neutron-induced fission cross section for incident neutron energies between 5 eV and 3.5 MeV

F. C. Difilippo,* R. B. Perez, G. de Saussure, D. K. Olsen, and R. W. Ingle
*Oak Ridge National Laboratory, P.O. Box X, Oak Ridge, Tennessee 37830*
(Received 4 June 1979)

A measurement of the $^{238}$U neutron-induced fission cross section has been performed in the neutron energy range between 5 eV and 3.5 MeV. The favorable signal-to-background ratio and high resolution of this experiment resulted in the identification of 85 subthreshold fission resonances or clusters of resonances in the neutron energy region between 5 eV and 200 keV. The fission data below 100 keV are characteristic of a weak coupling situation between Class I and Class II levels. The structure of the fission levels at the 720- and 1210-eV fission clusters is discussed. There is an apparent enhancement of the fission cross section at the opening of the $2^+$ neutron inelastic channel in $^{238}$U at 45 keV. An enhancement of the subthreshold fission cross section between 100 and 200 keV has been tentatively interpreted in terms of the presence of a Class II, partially damped vibrational level. There is a marked structure in the fission cross section above 200 keV up to and including the plateau between 2 and 3.5 MeV.

[NUCLEAR REACTIONS, FISSION $^{238}$U$(n,f)$. $E=5$ eV–3.5 MeV; measured $\sigma(E)$; deduced parameters second well fission barrier.]

## I. INTRODUCTION

Narrow intermediate structures in the subthreshold region of the neutron-induced fission cross section were first observed in $^{237}$Np by Paya *et al.*[1] and in $^{240}$Pu by Migneco and Theobald.[2] An interpretation of these structures was given independently by Weigmann[3] and by Lynn,[4] in terms of the double humped fission barrier proposed by Strutinsky.[5] According to this model the observed intermediate structure arises from the coupling between the Class I states corresponding to the ground-state deformation of the nucleus and the Class II states in the second minimum of the double humped fission barrier. Hence a study of subthreshold fission yields information on the shape of the potential barrier and on the nuclear states at high deformation, as discussed for instance in a recent review of neutron-induced fission by Michaudon.[6]

The $^{238}$U$(n,f)$ subthreshold fission is an interesting case of weak coupling between the levels of the two potential wells.[6] Although the existence of subthreshold fission in $^{238}$U has been known for a long time,[7] only recently has the intermediate structure been observed with good resolution and over an extended energy range.[8-12]

The $^{238}$U$(n,f)$ measurements presented here cover the energy region from 5 eV to 3.5 MeV with an energy resolution equal to or better than that of most previous measurements. More significant, in order to detect very weak fission levels, it is important to have a favorable signal-to-background ratio. Most of the background associated with measurements of subthreshold fission in $^{238}$U arises from fissions of $^{235}$U impurities in the $^{238}$U sample. The $^{238}$U sample used in the measurements presented here had an exceptionally high $^{238}$U isotopic purity[13] and had less than 2 ppm $^{235}$U.

The measurements were done by the time-of-flight technique, utilizing the ORELA facility[14] as a pulsed neutron source. The shape of the $^{238}$U to $^{235}$U fission ratio was obtained from the count rates of sections of the fission chamber containing either $^{238}$U or $^{235}$U. This fission ratio was normalized to a value $0.435 \pm 0.004$ for the interval from 2.35 to 2.95 MeV, the value obtained in a separate experiment described elsewhere.[15] The ENDF/B-IV description of the $^{235}$U$(n,f)$ cross

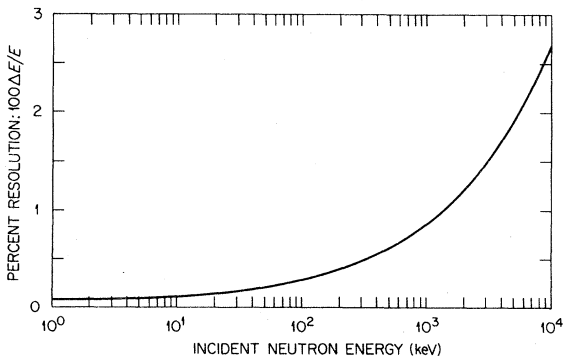


FIG. 1. Experimental energy resolution of the measurement. The resolution width $\Delta E$ is the computed $e$-folding Gaussian broadening width. Below 1 keV most of the broadening is due to the Doppler effect, $\Delta E_D = (4kTE/A)^{1/2}$, above 10 keV the broadening is mostly due to the Linac burst width of 30 ns: $\Delta E_T \approx 8.9 \times 10^{-6} E^{3/2}$, with $E$ in eV.

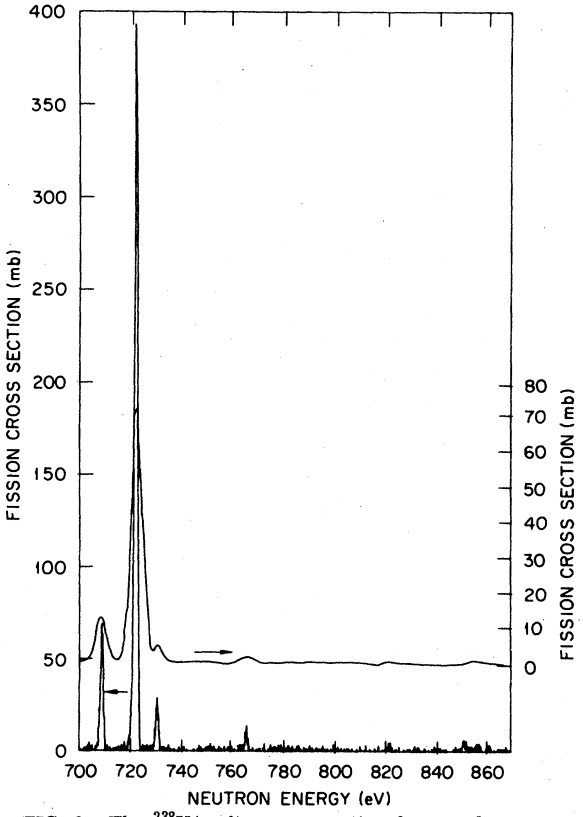


FIG. 2. The $^{238}$U($n,f$) cross section for incident neutron energies between 700 and 870 eV. The upper curve (right scale) shows our previously published low resolution data (Ref. 12), the lower curve (left scale) shows the present high resolution data. The improved resolution permits an unambiguous separation of the Class I resonances of the cluster centered at 720 eV.

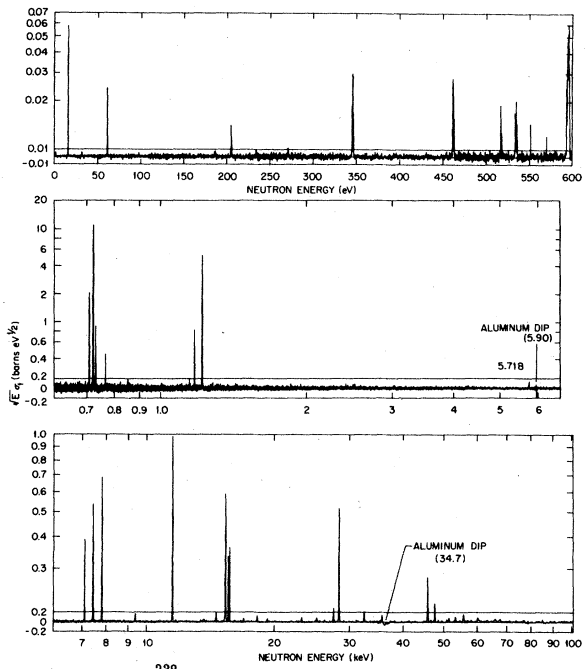


FIG. 3. The $^{238}$U($n,f$) cross section between 5 eV and 100 keV. The fission cross section has been multiplied by $E^{1/2}$ to keep the ordinate scale more uniform. Note that the ordinates change from linear to logarithmic scales. A few negative values, near 35 keV, result from a background overcorrection where aluminum has a large resonance distorting the incident neutron flux, and should be ignored.

section[16] was used to obtain the $^{238}$U($n,f$) cross section from the fission ratio.

A first experiment was done with a flight path of 20 m. The results of that measurement, the equipment and experimental techniques utilized have already been described[12] and hence will not be discussed here. In the present experiment the energy resolution was improved by the following: (1) the flight path was extended from 20 to 40 m, and (2) the time-of-flight spectra from the eight $^{238}$U sections of the fission chamber were stored separately and combined after correction for differences in flight path, whereas in our 20 m experiment[12] one common signal had been used for all eight sections.

The computed resolution width as a function of neutron energy for the 40 m experiment is given in Fig. 1. The effect of the improved resolution is illustrated in Fig. 2, where the data from our 20 and 40 m experiments are compared, in the range 700 to 870 eV.

In Sec. II the results of our 40 m experiment are presented in some detail and compared with previously reported data and with a recent evaluation of the $^{238}$U fission cross section.[17] In Sec. III we discuss some of the features of the observed cross section.

## II. RESULTS

The $^{238}$U($n,f$) cross section between 5 eV and 100 keV is shown in Fig. 3. The levels at 6.7, 20.9, and 36.7 eV had already been observed by Slovacek *et al.*,[9] but the good signal-to-background ratio of the present measurement permits the identification of 13 additional fission resonances between 40 and 600 eV. All the Class I levels in the clusters centered around 720 eV and 1.2 keV are well resolved. Between 5 and 100 keV 36 levels or clusters of levels have been identified.

In Fig. 4 the region 10 to 400 keV is shown in more detail. An enhancement of fission near 120 keV is tentatively interpreted as a contribution from a partially damped vibrational level centered near 145 keV with a width of about 65 keV. A similar structure was observed in the $^{234}$U($n,f$)

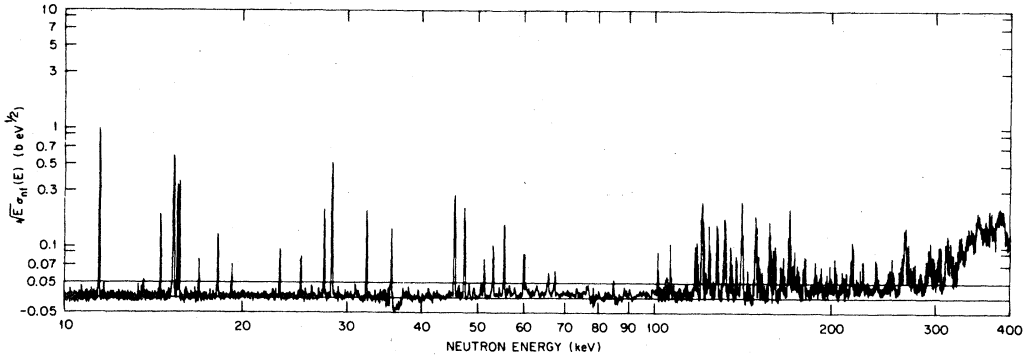


FIG. 4. The $^{238}U(n,f)$ cross section between 10 and 400 keV. The fission cross section has been multiplied by $E^{1/2}$ to keep the ordinate scale more uniform. Note that the ordinate is linear between $-0.05$ and $+0.05$ b eV$^{1/2}$ and logarithmic above 0.05 b eV$^{1/2}$. The negative values near 35 and 80 keV result from a background overcorrection where aluminum has large resonances distorting the incident neutron flux, and should be ignored. The fission strength enhancement between 120 and 170 keV is tentatively interpreted as resulting from a partially damped vibrational level centered near 145 keV.

cross section by James *et al.*[18]

The fission cross section between 100 keV and 1 MeV and between 0.4 and 3.6 MeV is shown in Figs. 5 and 6. A large number of measurements have been reported in that range, which have recently been reviewed by Poenitz *et al.*[17] who evaluated the fission cross section shown as the solid line in Figs. 5 and 6. The comparison indicates a good overall agreement between our data and the evaluation, however, our data show considerably more structure. This is not surprising because the evaluation is based on several data sets where the cross sections were averaged over intervals comparable to the widths of the structures. Our data agree qualitatively with those of Blons *et al.*[10] as reported by Cierjacks[19]; but the measurement of Blons *et al.*[10] has a somewhat better resolution in the high energy region and hence shows more structure.

The measured $^{238}U(n,f)$ cross section averaged over decimal energy intervals between 700 eV and 3 MeV is given in Table I. A total of 85 fission resonances or clusters of resonances have been identified below 200 keV. The fission areas of the 27 resolved resonances below 2 keV are listed in Table II. The areas of the 36 levels or clusters observed between 2 and 100 keV are listed in

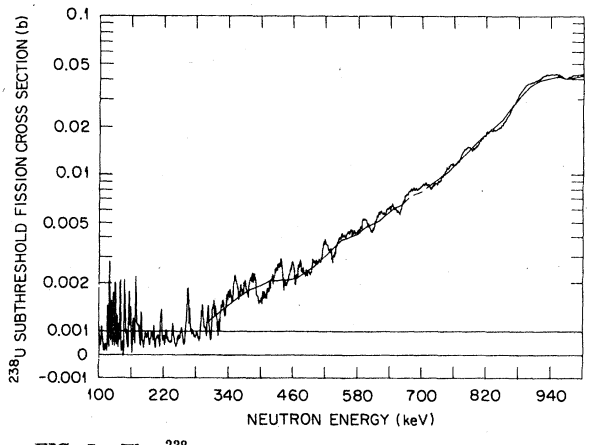


FIG. 5. The $^{238}U(n,f)$ cross section between 100 keV and 1.0 MeV. The smooth curve above 250 keV represents an evaluation of Poenitz *et al.* (Ref. 17). Note that the ordinate is linear from 0 to 0.001 b and logarithmic above 0.001 b.

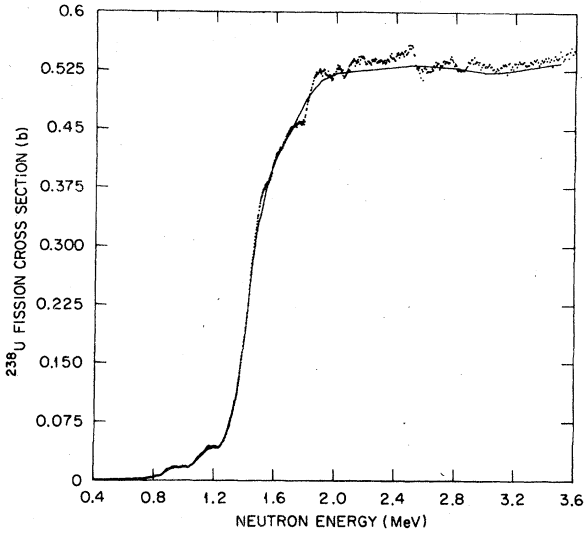


FIG. 6. The $^{238}U(n,f)$ cross section between 0.4 and 3.6 MeV. The smooth curve is an evaluation of Poenitz *et al.* (Ref. 17) based on a number of recent and older measurements (see text).

TABLE I. The $^{238}$U($n,f$) cross section averaged over decimal intervals between 0.7 keV and 3 MeV.

| Energy interval (keV) | $\sigma_f$, fission cross section [a] (mb) | Statistical error [b] (mb) |
|---|---|---|
| 0.7– 0.8 | 7.54 | 0.08 |
| 0.8– 0.9 | 0 | 0.005 |
| 0.9– 1.0 | 0 | 0.005 |
| 1.0– 2.0 | 0.390 | 0.007 |
| 2.0– 3.0 | 0 | <0.005 |
| 3.0– 4.0 | 0 | <0.005 |
| 4.0– 5.0 | 0 | <0.005 |
| 5.0– 6.0 | 0 | <0.005 |
| 6.0– 7.0 | 0 | <0.005 |
| 7.0– 8.0 | 0.42 | 0.01 |
| 8.0– 9.0 | 0 | <0.005 |
| 9.0– 10.0 | 0.05 | <0.005 |
| 10.0– 20.0 | 0.133 | <0.005 |
| 20.0– 30.0 | 0.086 | <0.005 |
| 30.0– 40.0 | 0.020 | <0.005 |
| 40.0– 50.0 | 0.088 | <0.005 |
| 50.0– 60.0 | 0.099 | <0.005 |
| 60.0– 70.0 | 0.0804 | <0.005 |
| 70.0– 80.0 | 0.0413 | <0.005 |
| 80.0– 90.0 | 0.0184 | <0.005 |
| 90.0– 100.0 | 0.0421 | <0.005 |
| 100.0– 200.0 | 0.099 | <0.005 |
| 200.0– 300.0 | 0.088 | <0.005 |
| 300.0– 400.0 | 0.199 | <0.005 |
| 400.0– 500.0 | 0.310 | <0.005 |
| 500.0– 600.0 | 0.640 | <0.005 |
| 600.0– 700.0 | 1.28 | <0.005 |
| 700.0– 800.0 | 2.76 | 0.005 |
| 800.0– 900.0 | 7.87 | 0.009 |
| 900.0–1000.0 | 16.58 | 0.02 |
| 1000.0–2000.0 | 283.0 | 0.1 |
| 2000.0–3000.0 | 536.0 | 0.2 |

[a] The $^{238}$U fission cross section was obtained from the measured ($^{238}$U/$^{235}$U) fission ratio, and the ENDF/B-IV representation of the $^{235}$U fission cross section.

[b] It is estimated that systematic errors amount to about 6%. These arise from uncertainties in normalization, in background substraction, and correction for scattering in the structural material of the detector.

Table III, and the areas of the 22 clusters identified between 100 and 200 keV are listed in Table IV. In Table III we have also listed the fission areas obtained in our previous experiment[12] at 20 m. The values given in Table IV of Ref. 12 were renormalized upward by 37%, for the following reason: As explained in Ref. 12 the fission areas were based on the assumption that the fission efficiencies of the $^{238}$U and $^{235}$U sections of the chamber were the same. No measurement of this fission ratio efficiency was then available. In the present experiment the fission areas could be obtained in absolute value by normalizing the $^{238}$U to $^{235}$U fission ratio in the interval 2.35 to 2.95 MeV and this yielded the value of the efficiency ratio.[15] The comparison of Table III shows that there is consistency between our present results and the renormalized 20 m results, but more clusters are observed with the better resolution available at 40 m.

The fission widths $\Gamma_f$ of the 27 resolved fission resonances below 2 keV have been obtained from the measured fission areas $A_f$ using the relation

$$A_f = \int \sigma_f dE = \frac{2\pi^2}{k^2} g \frac{\Gamma_f \Gamma_n}{\Gamma}, \quad (1)$$

where the symbols have the usual meaning.[20] For this calculation the values of the neutron width $\Gamma_n$ and total width $\Gamma$ were taken from our recent evaluation.[21] The values used for the neutron and total widths and the values obtained for the fission widths are also listed in Table II.

In Table V the fission cross sections areas obtained by several experimenters are compared. The discrepancies between the values are somewhat larger than expected.

## III. DISCUSSION

Figure 7 shows the cumulative sum of observed fission clusters as a function of neutron energy, up to 75 keV. Below 35 keV this cumulative sum can be fitted reasonably well by a straight line whose inverse slope corresponds to a spacing of $1.1 \pm 0.1$ keV. Between 45 and 55 keV the cumulative sum can again be fitted by a line of inverse slope corresponding to a spacing of $1.3 \pm 0.2$ keV. The uncertainties quoted are only sampling errors assuming a Wigner distribution of levels[22] [i.e., $(0.27D^2/N)^{1/2}$]. Between 37 and 45.5 keV there is a surprisingly large gap of about 8 keV with no observable level (see Figs. 3 and 4). (In fact the "gap" starts near 35.7 keV, but we estimate that between 35.7 and 37 keV small levels could be "obscured" by a large aluminum resonance which introduces a perturbation in the neutron flux incident upon our detector; see Fig. 4.) Above 60 keV the slope of the cumulative sum shown in Fig. 7 suggests that many levels are below the detection threshold of our measurements. Above 100 keV a new type of structure appears with relatively larger resonances having an average spacing of $3.3 \pm 0.4$ keV; we have already commented on this structure clearly visible in Fig. 4.

From the cumulative sum shown on Fig. 7 we estimate that the average Class II level spacing is of the order of 1 keV. We estimate that we may miss as much as 25% of the levels and that a realistic estimate of the Class II spacing at low energy may be $D_{II} = 1 \pm 0.25$ keV.

TABLE II. Measured fission areas and corresponding fission widths of 26 levels below 2 keV.

| Resonance energy [a] eV | Fission area [b] $10^{-6}$ b eV | Neutron widths [a] meV | Neutron reduced width [c] meV | Total widths [a] meV | Fission widths [b] neV |
|---|---|---|---|---|---|
| 6.672 | 376 ± 15 | 1.510 ± 0.015 | 0.58 ± 0.06 | 24.04 ± 0.62 | 9.7 ± 0.4 |
| 20.86 | 3290 ± 66 | 10.12 ± 0.10 | 2.22 ± 0.02 | 33.19 ± 0.46 | 55 ± 1 |
| 36.67 | 660 ± 40 | 33.91 ± 0.41 | 5.60 ± 0.07 | 56.83 ± 0.50 | 9.8 ± 0.6 |
| 66.02 | 1700 ± 70 | 24.61 ± 0.38 | 3.03 ± 0.05 | 48.30 ± 0.51 | 53 ± 2 |
| 80.73 | 233 ± 50 | 1.91 ± 0.04 | 0.213 ± 0.004 | 26.1 ± 1.2 | 62 ± 13 |
| 102.5 | 392 ± 78 | 71.64 ± 0.41 | 7.08 ± 0.04 | 96.05 ± 0.54 | 13 ± 3 |
| 189.6 | 690 ± 130 | 167.0 ± 1.7 | 12.1 ± 0.1 | 190.0 ± 1.8 | 36 ± 7 |
| 208.5 | 1120 ± 130 | 49.60 ± 0.79 | 3.44 ± 0.05 | 72.42 ± 0.89 | 83 ± 10 |
| 237.3 | 327 ± 95 | 26.48 ± 0.45 | 1.72 ± 0.03 | 51.23 ± 0.65 | 36 ± 11 |
| 347.8 | 2160 ± 170 | 81.73 ± 1.10 | 4.38 ± 0.06 | 104.5 ± 1.1 | 233 ± 20 |
| 376.9 | 73 ± 73 | 1.148 ± 0.024 | 0.059 ± 0.001 | 24.6 ± 2.4 | 140 ± 140 |
| 463.1 | 2370 ± 210 | 5.49 ± 0.15 | 0.255 ± 0.007 | 29.0 ± 2.4 | 1405 ± 150 |
| 478.4 | 300 ± 170 | 4.19 ± 0.10 | 0.192 ± 0.005 | 27.7 ± 2.4 | 230 ± 135 |
| 518.3 | 1250 ± 190 | 49.60 ± 0.75 | 2.18 ± 0.03 | 73.2 ± 0.9 | 232 ± 35 |
| 535.3 | 1860 ± 200 | 44.28 ± 0.74 | 1.91 ± 0.03 | 68.1 ± 0.79 | 370 ± 40 |
| 595.0 | 5550 ± 280 | 86.41 ± 1.32 | 3.54 ± 0.05 | 110 ± 1.3 | 1015 ± 50 |
| 619.9 | 550 ± 150 | 30.76 ± 0.51 | 1.24 ± 0.02 | 54.08 ± 0.64 | 144 ± 40 |
| 708.3 | 94 900 ± 2700 | 21.79 ± 0.59 | 0.82 ± 0.02 | 45.2 ± 0.81 | (33.8 ± 1.0) × $10^3$ |
| 721.6 | 611 400 ± 7200 | 1.72 ± 0.06 | 0.064 ± 0.002 | 25.2 ± 2.4 | (1570 ± 100) × $10^3$ |
| 730.1 | 35 600 ± 1700 | 0.93 ± 0.05 | 0.034 ± 0.002 | 24.4 ± 2.4 | (166 ± 10) × $10^3$ |
| 765.1 | 13 000 ± 1100 | 7.77 ± 0.28 | 0.28 ± 0.01 | 24.8 ± 2.0 | 7690 ± 780 |
| 821.6 | 900 ± 530 | 65.6 ± 1.3 | 2.29 ± 0.05 | 88.2 ± 1.4 | 240 ± 140 |
| 851.0 | 9250 ± 970 | 62.9 ± 1.5 | 2.16 ± 0.05 | 88.4 ± 1.7 | 2680 ± 280 |
| 856.1 | 5370 ± 700 | 86.2 ± 2.0 | 2.95 ± 0.07 | 109.7 ± 2.1 | 1420 ± 185 |
| 1140.0 | 7710 ± 860 | 233.1 ± 3.2 | 6.90 ± 0.09 | 256.9 ± 3.3 | 2350 ± 260 |
| 1168.0 | 43 500 ± 2100 | 87.7 ± 2.3 | 2.57 ± 0.07 | 111.8 ± 2.3 | (15.7 ± 0.8) × $10^3$ |
| 1211.0 | 341 300 ± 5700 | 9.19 ± 0.28 | 0.264 ± 0.008 | 32.7 ± 2.4 | (356 ± 20) × $10^3$ |

[a] Resonance energies, neutron widths, and total widths taken from Ref. 21.
[b] Fission areas and fission widths obtained from this experiment. Uncertainties given are statistical only.
[c] The neutron reduced widths were obtained assuming the levels to be $s$ wave.

In Fig. 8 the $^{238}U(n,f)$ cross section is compared to the $^{238}U(n,\gamma)$ cross section[23] over the range 20 to 100 keV. There is considerable evidence of intermediate structure in the $^{238}U(n,\gamma)$ cross section,[24] and the comparison shown on the figure was an attempt to determine if the intermediate structures in the fission and capture cross sections could be correlated. No significant "fine correlation" could be observed. Above 45 keV the capture cross section decreases because of the competition with the inelastic scattering channel corresponding to the first $2^+$ level in $^{238}U$; at 45 keV, there is a discontinuity in the derivative of the cross sections (Wigner cusp[25]) resulting in a rounded step[26] in the capture cross section (the cross section is slightly enhanced just below 45 keV and depressed just above.) Intuitively one would expect a similar behavior in the fission cross section. The data of Fig. 8 show that, on the contrary, the fission is weak below 45 keV and increases near 45 keV, a rather surprising result. It is also possible, of course, that the behavior of the subthreshold fission near 45 keV is not related to the opening of the inelastic channel.

## IV. INTERPRETATIONS OF THE CLUSTERS NEAR 720 AND 1210 eV

In this section we discuss several possible interpretations of the two clusters near 720 and 1210 eV.

The following approximate relations which can be derived by perturbation theory[3,4,27] are used:

$$T_A = 2\pi \frac{\Gamma_{II}(C)}{D_{II}} \tag{2}$$

$$T_B = 2\pi \frac{\Gamma_{II}(f)}{D_{II}} \tag{3}$$

$$\Gamma_{II}(C) = 2\pi \frac{\langle H^2 \rangle}{D_I} \tag{4}$$

$$\Gamma_{\lambda'}(f) = \frac{H^2_{\lambda''\lambda'}\Gamma_{\lambda II}(f)}{(E_{\lambda'} - E_{\lambda''})^2 + \frac{1}{4}W^2} \approx \frac{H^2_{\lambda''\lambda'}\Gamma_{\lambda II}(f)}{(E_{\lambda'} - E_{\lambda''})^2}, \tag{5}$$

where we use conventional notation. $T_A$ and $T_B$ represent the penetration through the inner and

TABLE III. Fission areas of clusters observed between 2 and 100 keV.

| This work | | Reference 12 [a] | |
|---|---|---|---|
| $E_0$ (keV) | Fission area [b] (b eV) | $E_0$ (keV) | Fission area [b] (b eV) |
| 5.718 | 0.025 ± 0.003 | 5.715 | 0.025 ± 0.002 |
| 7.098 | 0.075 ± 0.004 | 7.090 | 0.073 ± 0.004 |
| 7.427 | 0.176 ± 0.007 | 7.430 | 0.184 ± 0.008 |
| 7.799 | 0.162 ± 0.007 | 7.804 | 0.182 ± 0.008 |
| 9.348 | 0.047 ± 0.004 | 9.358 | 0.048 ± 0.004 |
| 11.441 | 0.316 ± 0.010 | 11.43 | 0.378 ± 0.038 |
| 11.661 [c] | 0.010 ± 0.002 | | |
| 13.578 [c] | 0.026 ± 0.003 | | |
| 14.507 | 0.065 ± 0.005 | 14.48 | 0.057 ± 0.005 |
| 15.252 | 0.346 ± 0.011 | 15.23 | 0.407 ± 0.011 |
| 15.496 [c] | 0.141 ± 0.007 | | |
| 15.594 | 0.343 ± 0.007 | 15.56 | 0.345 ± 0.010 |
| 16.839 [c] | 0.033 ± 0.004 | | |
| 18.107 | 0.079 ± 0.006 | 18.12 | 0.074 ± 0.004 |
| 19.145 [c] | 0.032 ± 0.004 | | |
| 23.028 | 0.063 ± 0.006 | 23.07 | 0.053 ± 0.005 |
| 25.006 | 0.045 ± 0.005 | 25.03 | 0.037 ± 0.005 |
| 26.105 | 0.020 ± 0.004 | 26.13 | 0.021 ± 0.004 |
| 27.399 | 0.150 ± 0.009 | 27.33 | 0.129 ± 0.011 |
| 28.215 | 0.389 ± 0.014 | 28.23 | 0.353 ± 0.021 |
| 30.940 | 0.016 ± 0.005 | 30.93 | 0.015 ± 0.003 |
| 32.322 | 0.160 ± 0.010 | 32.27 | 0.177 ± 0.013 |
| 35.614 | 0.090 ± 0.011 | 35.67 | 0.083 ± 0.008 |
| 45.575 | 0.318 ± 0.015 | 45.56 | 0.284 ± 0.019 |
| 46.381 [c] | 0.053 ± 0.006 | | |
| 47.408 | 0.248 ± 0.015 | 47.27 | 0.242 ± 0.019 |
| 48.289 [c] | 0.046 ± 0.006 | | |
| 49.169 [c] | 0.047 ± 0.006 | | |
| 50.562 | 0.053 ± 0.006 | 50.53 | 0.059 ± 0.009 |
| 51.222 | 0.100 ± 0.008 | 51.03 | 0.096 ± 0.016 |
| 52.763 | 0.155 ± 0.011 | 52.93 | 0.141 ± 0.014 |
| 54.259 | 0.041 ± 0.006 | | |
| 55.257 | 0.215 ± 0.013 | 55.29 | 0.259 ± 0.019 |
| 59.658 | 0.218 ± 0.013 | 56.40 [d] | 0.089 ± 0.008 |
| 65.658 [c] | 0.169 ± 0.012 | 57.40 [d] | 0.065 ± 0.010 |
| 67.451 [c] | 0.089 ± 0.009 | | |

[a] Renormalized: see text.
[b] Statistical error only.
[c] Cluster not observed in the work of Ref. 12.
[d] Cluster not observed in the present work.

TABLE IV. Fission areas of clusters observed between 100 and 200 keV.

| $E_0$ (keV) | Area (b eV) | Error [a] (b eV) |
|---|---|---|
| 112.9 | 0.106 | 0.013 |
| 117.2 | 0.387 | 0.038 |
| 119.9 | 0.669 | 0.046 |
| 121.8 | 0.123 | 0.019 |
| 123.0 | 0.282 | 0.024 |
| 124.8 | 0.093 | 0.019 |
| 127.2 | 0.443 | 0.039 |
| 131.1 | 0.610 | 0.040 |
| 133.9 | 0.303 | 0.026 |
| 137.1 | 0.210 | 0.017 |
| 140.0 | 0.600 | 0.043 |
| 143.6 | 0.126 | 0.018 |
| 147.7 | 0.503 | 0.032 |
| 149.7 | 0.183 | 0.023 |
| 151.5 | 0.129 | 0.017 |
| 156.1 | 0.526 | 0.029 |
| 159.1 | 0.362 | 0.030 |
| 164.3 | 0.430 | 0.025 |
| 168.9 | 0.749 | 0.038 |
| 172.1 | 0.214 | 0.018 |
| 174.5 | 0.345 | 0.028 |
| 178.9 | 0.327 | 0.018 |

[a] Statistical error only, systematic errors arising from uncertainties in normalization, background correction, and identification of the cluster limits are estimated to amount to 8%.

outer potential barriers, respectively; $D_{\mathrm{I}} \approx 25$ eV the Class I average level spacing, $D_{\mathrm{II}} \approx 1000$ eV and Class II average level spacing. $\Gamma_{\mathrm{II}}(C)$ is the spreading or coupling width; $\Gamma_{\mathrm{II}}(f)$ the escape width; $\langle H^2 \rangle$ is the average value of the square coupling matrix element, $H^2_{\lambda''\lambda'}$, between the Class I level $\lambda'$ and the Class II level $\lambda''$. $\Gamma_{\lambda'}(f)$ represents the fission width of the Class I level at energy $E_{\lambda'}$, and $\Gamma_{\lambda\mathrm{II}}(f)$ the fission width of the quasi-Class II level at $E_{\lambda''}$. The total width of a Class II state, $W$, is $W \approx \Gamma_{\mathrm{II}}(f) + \Gamma_{\mathrm{II}}(C) + \Gamma_{\mathrm{II}}(\gamma)$.

In Figs. 9, 10, and 11 the fission cross section is compared to the effective capture cross section[23] over the ranges 5 to 400 eV, 600 to 900 eV and 1.1 to 1.3 keV, respectively. The purpose of showing the capture data in these figures is to locate the position of the large $s$-wave levels. Great care was taken in "aligning" the energy scales of the two measurements. This was done using the 6.67 eV level and the dip near 5.9 keV due to an aluminum resonance. We estimate that the relative energy alignment of our capture and fission data cannot be in error by more than 1 eV at 1 keV. This alignment is confirmed by the observation that the 27 fission resonances below 2 keV, listed in Table II, all line up to better than ±1 eV with resonances in the capture data. We will examine the two alternative hypotheses $T_A > T_B$ or $T_B > T_A$ and show that both can be made consistent with the observed data.

First we assume that $T_A > T_B$, that is, that the transmission of the inner barrier is larger than that of the outer barrier, and hence that the spreading width $\Gamma_{\mathrm{II}}(C)$ is larger than the escape width $\Gamma_{\mathrm{II}}(f)$. As shown by Weigmann *et al.*,[28] the Class II state is then mixed into the fine structure resonances so that the following sum rule

TABLE V. Comparison of fission areas obtained by several experimenters. [a]

| Resonance energy (eV) | RPI (Ref. 8) | RPI (Ref. 9) | Geel (Ref. 11) | ORNL [b,c] (Ref. 12) | This work [c] |
|---|---|---|---|---|---|
| 6.672 | | $(340 \pm 39) \times 10^{-6}$ | | | $(376 \pm 15) \times 10^{-6}$ |
| 20.86 | | $(2880 \pm 320) \times 10^{-6}$ | | | $(3290 \pm 66) \times 10^{-6}$ |
| 36.67 | | $(771 \pm 97) \times 10^{-6}$ | | | $(660 \pm 40) \times 10^{-6}$ |
| 708.3 | | | <0.07 | 0.094 ± 0.007 | 0.0948 ± 0.0027 |
| 721.6 | 0.31 ± 0.08 | | 0.26 ± 0.04 | 0.56 ± 0.02 | 0.611 ± 0.007 |
| 730.1 | | | <0.03 | 0.026 ± 0.002 [e] | 0.036 ± 0.002 |
| 765.1 | | | <0.05 | 0.013 ± 0.002 | 0.013 ± 0.002 |
| 1108 | | | 0.05 ± 0.02 | | N.O. [d] |
| 1140 | | | 0.13 ± 0.05 | 0.007 ± 0.001 | 0.008 ± 0.001 |
| 1168 | | | 0.07 ± 0.04 | 0.042 ± 0.004 | 0.043 ± 0.002 |
| 1176 | | | 0.06 ± 0.03 | | N.O. |
| 1194 | | | 0.07 ± 0.03 | | N.O. |
| 1211 | 0.11 ± 0.03 | | 0.20 ± 0.04 | 0.35 ± 0.02 | 0.341 ± 0.006 |

[a] All areas are given in b eV.
[b] Renormalized (see text).
[c] Uncertainty given is statistical only (1 SD).
[d] N.O. for not observed.
[e] This level was not fully resolved in the work of Ref. 12; see Fig. 2.

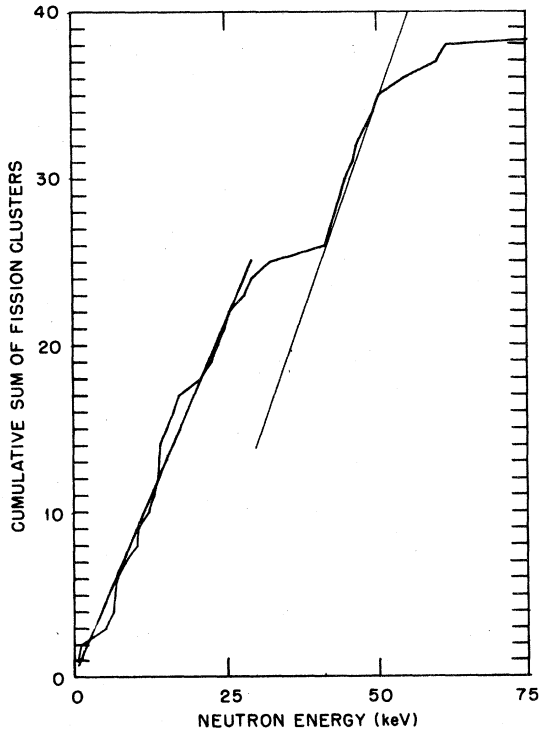


FIG. 7. Cumulative number of fission clusters observed versus incident neutron energy. The 38 clusters are listed in Tables II and III and indicated in Fig. 3. The experimental resolution does not permit to resolve the Class I levels above a few keV. The slopes correspond to Class I spacings of 1.1 keV below 35 keV and 1.3 keV above 45 keV. Above 55 keV a large number of clusters are probably not detected or not resolved. Note the discontinuity between 35 and 45 keV.

applies:

$$\Gamma_{\lambda II}(f) = \sum_{\lambda'} \Gamma_{\lambda'}(f), \qquad (6)$$

where the sum is over the observed resonances of

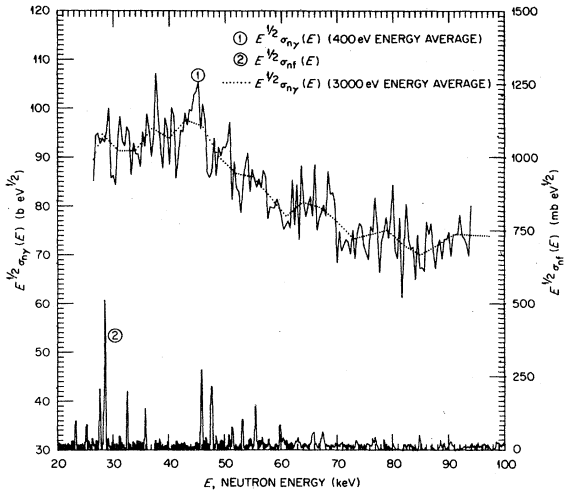


FIG. 8. Comparison of the $^{238}U(n,f)$ cross section (lower curve, right-hand side scale) with the $^{238}U(n,\gamma)$ cross section (upper curve, left-hand side scale). Both cross sections have been multiplied by $E^{1/2}$ to keep the ordinate scale more uniform. The capture cross section is shown averaged over two different energy widths: the capture data averaged over 3 keV wide intervals illustrate the "long-range behavior" of the cross section. Above 45 keV the capture decreases because of the competition with the inelastic scattering channel corresponding to the first $2^+$ level in $^{238}U$. Instead the fission is enhanced above 45 keV (see text).

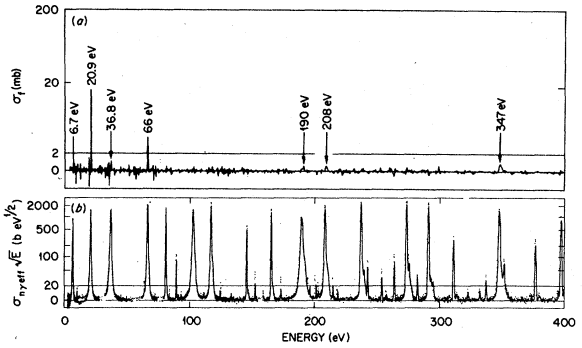


FIG. 9. Comparison of the $^{238}$U$(n,f)$ and $^{238}$U$(n,\gamma)$ cross sections for incident neutron energies between 5 and 400 eV. The effective capture cross section (Ref. 23) is not corrected for selfshielding and multiple scattering and has been multiplied by $E^{1/2}$. The capture data help in locating the position of the $s$-wave levels. Note that the ordinates change from linear to logarithmic scales. The areas of the fission resonances are given in Table II.

a cluster. The resonance which carries the largest fission width, called the "central resonance," is the quasi-Class II state.

Using Eq. (6) and the values of $\Gamma_{\lambda'}(f)$ of Table II

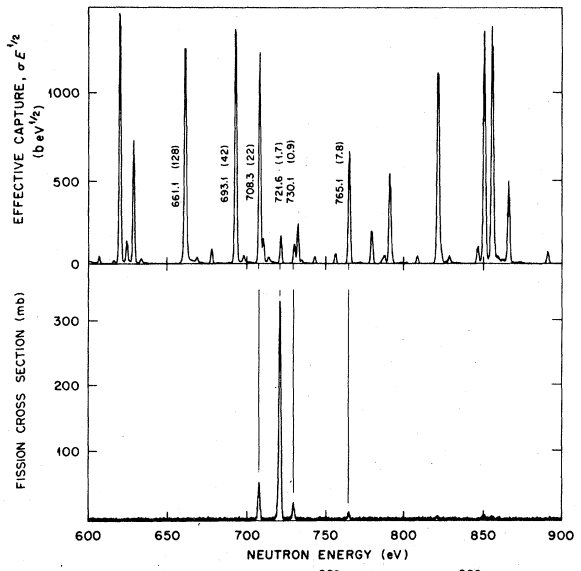


FIG. 10. Comparison of the $^{238}$U$(n,f)$ and $^{238}$U$(n,\gamma)$ cross sections for incident neutron energies between 600 and 900 eV. The effective capture cross section (Ref. 23) is not corrected for selfshielding and multiple scattering and has been multiplied by $E^{1/2}$. The resonance energies in eV and neutron widths in meV are from our recent evaluation (Ref. 21). Note that all the fission resonances are aligned with well-known $s$-wave levels. The areas of the fission resonances are given in Table II.

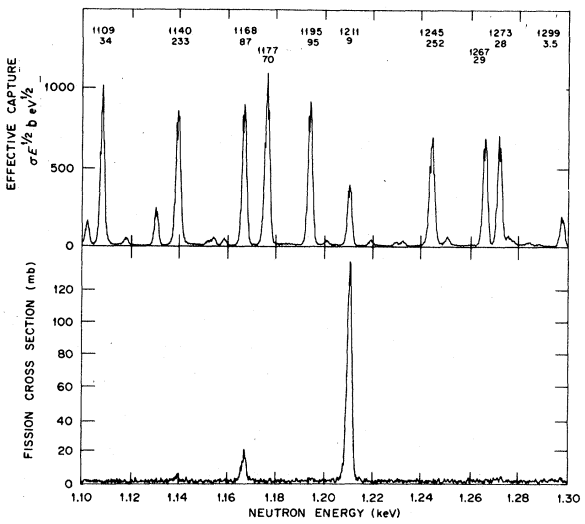


FIG. 11. Comparison of the $^{238}$U$(n,f)$ and $^{238}$U$(n,\gamma)$ cross sections for incident neutron energies between 1.1 and 1.3 keV. The effective capture cross section (Ref. 23) is not corrected for selfshielding and multiple scattering and has been multiplied by $E^{1/2}$. The resonance energies in eV and neutron widths in meV are from our recent evaluation (Ref. 21). The areas of the fission resonances are given in Table II.

we obtain values of 1.8 meV and 0.4 meV for $\Gamma_{\lambda II}(f)$ near 722 and 1211 eV, respectively. By using Eq. (5) we can derive estimates of $H_{\lambda''\lambda'}{}^2$ of 3 (eV)$^2$ for the cluster near 722 eV and 16 (eV)$^2$ for the cluster near 1211 eV. The values of $H_{\lambda''\lambda'}{}^2$ are listed in Tables VI and VII. Hence we estimate $\langle H^2\rangle \approx 10$ (eV)$^2$ leading to a value $\Gamma_{II}(C) \approx 2$ eV, by Eq. (4), and by Eqs. (2) and (3) to the estimates $T_A \approx 1.2\times10^{-2}$ and $T_B \approx 6.10^{-6}$.

Back *et al.*[29] have estimated the parameters of the double hump fission barrier of actinides on the basis of measurements of fission probabilities and of a study of the systematic trends of these parameters with respect to $A$ and $Z$. For the compound nucleus $^{239}$U their estimates are given in the second and third columns of Table VIII. The last column of the table gives the transmission of each barrier for neutrons of total energy near the binding energy $S_n = 4.81$ MeV. These transmissions were computed by the usual expression:

$$T = \left\{1 + \exp\left[\frac{2\pi}{\hbar\omega}(V - S_n)\right]\right\}^{-1}. \quad (7)$$

Our estimate of the outer barrier transmission is consistent with that derived from the parameters of Back *et al.*, however, for the inner barrier our value is larger by more than three orders of magnitude.

The neutron width of the quasi-Class II states

TABLE VI. Calculation of average square coupling matrix element (near level at 721.6 eV).

| $E_{\lambda'}$ eV | $\Gamma_{\lambda'}(f)$ [a] meV | $(E_{\lambda'}-721.6)^2\Gamma_{\lambda'}(f)$ $(eV)^3$ | $H_{\lambda'\lambda''}^2$ for $\Gamma_{\lambda II}(f)=1.8$ meV $(eV)^2$ |
|---|---|---|---|
| 595.0 | 0.001 015 | 0.0163 | 9.1 |
| 619.9 | 0.000 144 | 0.0015 | 0.8 |
| 628.5 | <0.000 07 | 0.0003 | 0.2 |
| 661.1 | <0.000 003 | 0.0 | 0 |
| 693.1 | <0.000 01 | 0.0 | 0 |
| 708.3 | 0.033 8 | 0.0060 | 3.3 |
| (721.6) | (1.57) | | |
| 730.1 | 0.166 | 0.0120 | 6.7 |
| 765.1 | 0.007 69 | 0.0146 | 8.1 |
| 790.8 | <0.000 07 | 0.0002 | 0.1 |
| Average: | | 0.0056 | 3.1 |

[a] Where $\Gamma_{\lambda'}(f)$ was not measured, an upper limit was computed assuming a minimum detectable fission area of $10^{-4}$ b eV. The probable value was then taken as half that upper limit.

can also be estimated by perturbation theory:

$$\Gamma_{\lambda II}(n) \approx \frac{D_{II}}{D_I}\frac{\Gamma_I(n)}{4}T_A, \tag{8}$$

where $\Gamma_I(n)$ is the average neutron width of nearby Class I states. The value obtained, ~11 meV, is quite consistent with the values 1.7 meV and 9.2 meV evaluated for the central resonance of the clusters near 721 and 1211 eV, respectively.

If we now instead assume that $T_B > T_A$, i.e., that the transmission of the outer barrier is larger, then, again according to Weigmann *et al.*,[29] the quasi-Class II state is a very broad state, essentially unobservable in neutron induced reactions because of its large total width and small neutron width. For the observed resonances of a cluster we now have

$$\Gamma_{\lambda II}(C) = \sum_{\lambda'} \Gamma_{\lambda'}(f). \tag{9}$$

From the values of Table II we now derive values of 1.8 meV and 0.4 meV for $\Gamma_{\lambda II}(C)$ for the two clusters, and by Eq. (4) we obtain $\langle H^2\rangle \approx 4.10^{-3}$ $(eV)^2$. From the values of Tables VI and VII we now derive $\Gamma_{II}(f) \approx 2$ eV, and by Eqs. (1) and (2) we have $T_A \approx 6.10^{-6}$ and $T_B \approx 1.2\times 10^{-2}$. This time our value of $T_A$ is consistent with that derived from the parameters of Back *et al.*, but our value of $T_B$ is larger by several orders of magnitude.

Hence our analysis does not let us decide between the two possibilities $T_A > T_B$ or $T_B > T_A$. In either case our estimated transmission of one barrier is consistent with that derived from the parameters of Back *et al.*, while our estimated transmission of the other barrier is considerably larger.

Weigmann *et al.*[28] have argued that the gamma-ray spectrum of neutron capture in a predominantly Class II level should be softer than that of a Class I level. Their study of the gamma-ray spectra of the levels at 722 and 1211 eV indicated

TABLE VII. Calculation of average square coupling matrix element (near level at 1211 eV).

| $E_{\lambda'}$ eV | $\Gamma_{\lambda'}(f)$ [a] meV | $(E_{\lambda'}-1211)^2\Gamma_{\lambda'}(f)$ $(eV)^3$ | $H_{\lambda\lambda'}^2$ for $\Gamma_{II}(f)=0.4$ meV $(eV)^2$ |
|---|---|---|---|
| 1109 | <0.000 02 | 0.000 104 | 0.26 |
| 1140 | 0.002 35 | 0.011 85 | 29.6 |
| 1168 | 0.015 7 | 0.029 03 | 72.6 |
| 1177 | <0.000 01 | 0.000 006 | 0.015 |
| 1195 | <0.000 01 | 0.000 001 | 0.0025 |
| (1211) | (0.356) | | |
| 1245 | <0.000 003 | 0.000 002 | 0.005 |
| 1267 | 0.004 | 0.012 54 | 31.35 |
| 1273 | <0.000 02 | 0.000 04 | 0.10 |
| 1299 | <0.000 2 | 0.000 75 | 1.9 |
| Average: | | 0.006 | 16 |

[a] Where $\Gamma_{\lambda'}(f)$ was not measured, an upper limit was computed assuming a minimum detectable fission area of $10^{-4}$ b eV. The probable value was then taken as half that upper limit.

TABLE VIII. Estimated (Ref. 29) barrier parameters for $^{239}$U ($S_n = 4.81$ MeV, neutron binding energy).

| Barrier | $V$/MeV | $\hbar\omega$/MeV | $\frac{2\pi}{\hbar\omega}(V - S_n)$ | Transmission |
|---|---|---|---|---|
| Inner | 6.55 ± 0.30 | 0.90 | 12.14 ± 2.10 | $5.3 \times 10^{-6}$ |
| Outer | 6.30 ± 0.30 | 0.65 | 14.40 ± 2.90 | $5.5 \times 10^{-7}$ |

that these spectra were consistent with those of other Class I levels and inconsistent with the spectra expected from Class II levels; hence these authors concluded that the levels near 722 and 1211 eV were essentially Class I levels. Browne[30] has also investigated the gamma-ray spectrum of the 722 eV level and, contrary to Weigmann *et al.*, he finds this spectrum significantly softer than that of nearby Class I levels and concludes that the 722 eV level is almost pure Class II. There is clearly a need for additional work to resolve this discrepancy.

As can be seen in Fig. 9 and in Table II, several $s$-wave levels dispersed throughout the resolved resonance region exhibit subthreshold fission with small but significant fission widths. The width corresponding to direct penetration through the double humped fission barrier was estimated using the expression given by Gai *et al.*,[31] $\Gamma_{min} = D_I T_A T_B / 8\pi$, where $T_A$ and $T_B$ represent the transmission through the first and second barrier, respectively.

If the transmissions are computed with the parameters of Back *et al.*, a value $\Gamma_{min} \approx 10^{-11}$ eV is obtained, which is a few orders of magnitude smaller than the values in the range $10^{-8}$ to $2.5 \times 10^{-7}$ eV observed for some levels in the range 5 to 600 eV. However, if the transmission derived from our analysis are used, $T_A \times T_B \approx 10^{-7}$ and $\Gamma_{min} \approx 10^{-7}$ eV. This value is in good agreement with the measured fission widths of some levels in the range 5 to 600 eV.

Before concluding this section we note that the quasi-Class II state may decay by gamma transitions to the lowest state in the second well of the potential barrier, resulting in the formation of a shape isomer of $^{239}$U. In the hypothesis $T_A > T_B$ this shape isomer would mostly decay to the ground state of $^{239}$U by gamma-ray transition. On the other hand if $T_B > T_A$ the shape isomer would result in delayed fission. However, since in this case we estimate an escape width of the order of 2 eV and a width for gamma transition to the shape isomer of the order of 20 meV at most, the branching ratio for formation of this shape isomer is small. To our knowledge no spontaneously fissioning isomer of $^{239}$U has been reported.

## V. CONCLUSIONS

We present the results of good resolution, low background measurements of the $^{238}$U$(n,f)$ cross section from 5 eV to 3.5 MeV. The subthreshold region of the cross section is rich with structures which vary with the incident neutron energy. At the opening of the inelastic scattering channel near 45 keV there is a discontinuity in the derivative of the cross section. One would expect the subthreshold fission to decrease just above 45 keV, due to the competition with the new channel; instead a marked and sudden increase is observed.

Below 30 keV the subthreshold fission cross section shows the characteristic pattern of a very weak coupling between the Class I and Class II states. A value $D_{II} = 1 \pm 0.25$ keV is obtained for the Class II level spacing.

Two possible interpretations of the well-known clusters centered near 720 and 1210 eV are discussed. Our analysis does not let us determine uniquely the transmission of the two humps of the double humped fission barrier. But the product of these two transmissions, as obtained from our analysis, is a few orders of magnitude larger than that obtained from the barrier parameters of Back *et al.* A small but significant fission width can be measured for many of the low energy $s$-wave levels. These widths are consistent with the product of the barrier transmission as obtained from our analysis.

## ACKNOWLEDGMENTS

We are indebted to the ORNL Thermonuclear Division for the loan of a $^{238}$U fission chamber with unusually high isotopic purity, and to F. Gillespie for preparing this chamber. We are also indebted to H. Todd and the ORELA staff for the operation of the Linac, to J. G. Craven for his help with the ORELA data acquisition system, and to H. Weaver for his considerable assistance in the installation of the equipment. Finally, we are indebted to R. L. Macklin, R. W. Peelle, and S. Raman for many fruitful discussions. This research was sponsored by the Department of Energy under Contract W-7405-eng-26 with the Union Carbide Corporation. F.C.D. was supported by an IAEA Fellowship.

*Present address: Comision Nacional de Energia Atomica, Argentina.

[1]D. Paya, H. Derrien, A. Fubini, A. Michaudon, and P. Ribon, *Proceedings of the Conference on Nuclear Data, Microscopic Cross Sections and Other Data Basic to Reactors, Paris, 1966* (International Atomic Energy Agency, Vienna, Austria, 1967), Vol. II, p. 128.

[2]E. Migneco and J. P. Theobald, Nucl. Phys. A112, 603 (1968).

[3]H. Weigmann, Z. Phys. 214, 7 (1968).

[4]J. E. Lynn, U. K. Atomic Energy Authority, Harwell, Report No. AERE-R5891 (1968); see also J. E. Lynn, *Proceedings of the Second IAE Symposium on Physics and Chemistry of Fission, Vienna, Austria, 1969* (International Atomic Energy Agency, Vienna, Austria, 1969), p. 249.

[5]V. M. Strutinsky, Nucl. Phys. A95, 420 (1967); A122, 1 (1968).

[6]A. Michaudon, *Proceedings of the International Conference on the Interactions of Neutrons with Nuclei*, Lowell, Mass., July 6–9, 1976, Report No. CONF-760715-PI, Vol. 1, p. 641.

[7]M. G. Silbert and D. W. Bergen, Phys. Rev. C 4, 220 (1971).

[8]R. C. Block, R. W Hockenbury, R. D. Slovacek, E. B. Bean, and D. S. Cramer, Phys. Rev. Lett. 31, 247 (1973).

[9]R. E. Slovacek, D. S. Cramer, E. B. Bean, R. W. Hockenbury, J. R. Valentine, and R. C. Block, Bull. Am. Phys. Soc. 20, 581 (1975). See also R. E. Slovacek, D. S. Cramer, E. B. Bean, J. R. Valentine, R. W. Hockenbury, and R. C. Block, Nucl. Sci. Eng. 62, 455 (1977).

[10]J. Blons, C. Mazur, and D. Paya, *Proceedings of the Conference on Nuclear Cross Sections and Technology*, Washington D. C., March 3–7 1975, edited by R. Schranck and C. D. Bowman (National Bureau of Standards Special Publication No. 425, 1975), p. 642.

[11]J. A. Wartena, H. Weigmann, and E. Migneco, *Proceedings of the Conference on Nuclear Cross Sections and Technology*, Washington D.C., March 3–7, 1975, edited by R. C. Schranck and C. D. Bowman (National Bureau of Standards Special Publication No. 425, 1975), p. 597.

[12]F. C. Difilippo. R. B. Perez, G. de Saussure, D. K. Olsen, and R. W. Ingle, Trans. Am. Nucl. Soc. 23, 499 (1976); Nucl. Sci. Eng. 63, 153 (1977).

[13]We are indebted to the ORNL Thermonuclear Division for the loan of this high purity sample.

[14]F. C. Maienschein, Energ. Nucl. 79, 533 (1972) (English translation in Oak Ridge National Laboratory Report No. ORNL-TM-3833, 1972) (unpublished).

[15]F. C. Difilippo. R. B. Perez, G. de Saussure, D. K. Olsen, and R. W. Ingle, Nucl. Sci. Eng. 68, 43 (1978).

[16]Evaluated Nuclear Data File, Version IV, of the National Neutron Cross Section Center. Principal evaluators for $^{235}$U are L. Stewart, H. Alter, and R. Hunter, (Brookhaven National Laboratory, Upton, New York).

[17]W. Poenitz, E. Pennington, A. B. Smith, and R. Howerton, Argonne National Laboratory Report No. ANL/NDM-32, 1977 (unpublished). See also, Supplement to Report No. ANL-76-90, Proceedings of the NEANDC/NEACRP Specialists Meeting on Fast Neutron Fission Cross Sections of U-233, U-235, U-238, and Pu-239, June 28–30, 1976, edited by W. P. Poenitz and A. B. Smith (U. S. Department of Commerce, Argonne, Illinois, 1976) where many of the recent measurements of the $^{238}$U($n$, $f$) cross section are compared.

[18]G. D. James, J. W. T. Dabbs, J. A. Harvey, N. W. Hill, and R. H. Schindler, Phys. Rev. C 15, 2083 (1977).

[19]S. Cierjacks, in *Neutron Standards and Applications, Proceedings of a Symposium* (National Bureau of Standard Special Publication No. 493, Washington, D.C., 1977), p. 278.

[20]See for instance, *Experimental Neutron Resonance Spectroscopy*, edited by J. A. Harvey (Academic, New York, 1970).

[21]G. de Saussure, D. K. Olsen, R. B. Perez, and F. C. Difilippo, *Progress in Nuclear Energy* (Pergamon, New York, 1979), Vol. 3, pp. 87–124.

[22]E. P. Wigner, in *Proceedings of the Conference on Neutron Physics by Time-of-Flight*, Gatlinburg, Tennessee, 1956 [Oak Ridge National Laboratory Report No. ORNL-2309 (unpublished)].

[23]G. de Saussure, E. G. Silver, R. B. Perez, R. Ingle, and H. Weaver, Nucl. Sci. Eng. 51, 385 (1973).

[24]R. R. Spencer and F. Kaeppeler, *Proceedings of the Conference on Nuclear Cross Sections and Technology, Washington D. C., March 3–7, 1975*, edited by R. C. Schranck and C. D. Bowman (National Bureau of Standards Special Publication No. 425, 1975), p. 620; also R. B. Perez, G. de Saussure, R. L. Macklin, and J. Halperin, Phys. Rev. C 20, 528 (1979).

[25]E. P. Wigner, Phys. Rev. 73, 1002 (1948).

[26]R. G. Newton, *Scattering Theory of Waves and Particles* (McGraw-Hill, New York, 1966), p. 533.

[27]J. E. Lynn, Harwell Report Nos. UKNDC-NSC (74), p. 2, and NEANDC(UK) 162 AL (unpublished).

[28]H. Weigmann, G. Rohr, T. Vander Veen, G. Vanpraet, in *Proceedings of the Second International Symposium on Neutron Capture Gamma-Ray Spectroscopy and Related Topics, Petten, 1974* (Reactor Centrum Nederland, Petten, 1975), p. 673.

[29]B. B. Back, O. Hansen, G. C. Britt, J. D. Garrett, and B. Leroux, in *Proceedings of the Third International Atomic Energy Symposium on the Physics and Chemistry of Fission, Rochester, 1973* (International Atomic Energy Agency, Vienna, 1974), p. 3.

[30]J. C. Browne, Vol. II, p. 1402, *Proceedings of the International Conference on the Interaction of Neutron with Nuclei*, Lowell, Mass., July 6–9, 1976, p. 2, T. I. C., ERDA.

[31]E. V. Gai, A. V. Ignatuk, N. K. Rabotnov, and G. N. Smirenkin, *Proceedings of the Second International Atomic Energy Symposium on Physics and Chemistry of Fission, Vienna, Austria, 1969* (IAEA, Vienna, 1969).